Thermal, optical and structural properties of blocks and blends of PLA and P2HEB

ice | science

ice Institution of Civil Engineers publishing

Thermal, optical and structural properties of blocks and blends of PLA and an aromatic/aliphatic polyester

Vishalkumar A. Makwana, MSc

Ph.D. Student, EaStCHEM School of Chemistry. University of Edinburgh, Joseph Black Building, David Brewster Rd, Edinburgh EH9 3FJ, ORCID number

Erlantz Lizundia*, Ph.D.

BCMaterials, Basque Center for Materials, Applications and Nanostructures, UPV/EHU Science Park, 48940 Leioa, Spain, ORCID number: 0000-0003-4013-2721

Aitor Larrañaga, Ph.D.

Advanced technician, SGIker, General Research Services, University of the Basque Country (UPV/EHU), Spain. ORCID number

José Luis Vilas, Ph.D.

Professor, Macromolecular Chemistry Research Group. Department of Physical Chemistry. Faculty of Science and Technology. Basque Centre for Materials, Applications and Nanostructures (BCMaterials), Parque Tecnológico de Bizkaia, Ed. 500, 48160 Derio, Spain, ORCID number

Michael P. Shaver*, Ph.D.

Personal Chair in Polymer Chemistry, EaStCHEM School of Chemistry. University of Edinburgh, Joseph Black Building, David Brewster Rd, Edinburgh EH9 3FJ, ORCID number

***Corresponding Author**

Dept. of Graphic Design and Engineering Projects, University of the Basque Country (UPV/EHU), 48013 Bilbao – Spain, Phone: +34 94 601 3965, E-mail address: erlantz.liizundia@ehu.eus

EaStCHEM School of Chemistry, University of Edinburgh, Joseph Black Building, David Brewster Rd, Edinburgh EH9 3FJ, Phone: +0131 650 4726, E-mail address: michael.shaver@ed.ac.uk

Biodegradable diblock and triblock copolymers and blends were prepared, consisting of poly(L-lactic acid) and an aromatic/aliphatic polyester mimicking polyethylene phthalate. As poly(2-(2-hydroxyethoxy)benzoate) possesses unique degradability and thermal properties, these novel block copolymers were explored through thermal analysis, UV-Vis spectroscopy, X-ray diffraction and comparative enzymatic and catalytic degradation. Poly(L-lactic acid), the product of ring opening polymerization of L-lactide by an aluminium salen catalyst, was used as a macroinitiator in the ring opening polymerization of 2,3-dihydro-5H-1,4-benzodioxepin-5-one to afford target diblock and triblock copolymers. Copolymerization dramatically improved the thermal and optical properties of poly(2-(2-hydroxyethoxy)benzoate), especially in comparison to polymer blends which favored non-interacting phases that worsened properties. The chemical and enzymatic degradation profiles of the copolymers were studied by depolymerizing with the aforementioned aluminium salen catalyst and degrading with proteinase K.

Keywords: Biodegradable polymers, poly(lactic acid), thermal properties

1. Introduction

The rapid increase in plastic waste has led to growing interest in biodegradable polymers in both academic and industrial research, evidenced by significant commercial growth of this sector.[1] Biodegradable polymers, and more specifically aliphatic polyesters, are now well established and widely used in biomedicine,[2] agriculture,[3] pharmacology[4] and ecology.[5]

Flagship polymers poly(lactic acid) (PLA), poly(ε-caprolactone) (PCL), poly(lactic-co-glycolic acid) (PLGA), and poly-3-hydroxybutyrate (PHB) each have characteristic hydrolytic, enzymatic, and catalytic degradability.[6, 7] They are often prepared through ring opening polymerization (ROP) of a cyclic ester; in the case of PLA the cyclic diester lactide is used.[8] PLA has glass transition temperatures (T_g) from 40–70 °C and a melting temperature (T_m) from 130–180 °C depending on the tacticity and molecular weight. These thermal properties, its inherently brittle nature and high permeability to ultraviolet (UV) light limit its application.[9] Additionally, while PLA is degraded through industrial enzymatic composting into lactic acid, the energy intensive process and required reformation of the diester do limit sustainability.[10-12]

We have recently reported the synthesis and characterization of an aromatic-aliphatic polyester, poly(2-(2-hydroxyethoxy) benzoate) (P2HEB).[13, 14] The ROP of 2,3-dihydro-5H-1,4-benzodioxepin-5-one (2,3-DHB), mediated by an aluminium salen catalyst, has a finely tunable monomer-polymer equilibrium, resulting in polymerization to high molecular weight, narrow dispersity P2HEB and selective depolymerization back to the cyclic monomer under dilute conditions.[14] Closing the loop on these polymerizations suggest a new recycling strategy that avoids inefficient biodegradation in favour of chemical and thermal recovery of monomers.[12] P2HEB has a T_g of 27 °C and a T_m of 80 °C, mimicking that of the ortho-linked poly(ethylene phthalate).[13] It has a low crystallizability and a storage modulus of 1050 MPa.[13] These thermal and mechanical properties limit the application range of P2HEB as a homopolymer, yet suggest potentially interesting uses in copolymers. Coupled with its advantageous UV absorbance and degradation profile, we sought to explore this key monomer in both block copolymerization and polymer blends with PLA.

Various methods have been implemented to improve the properties of PLA, whilst maintaining its sustainability, including: composite fabrication,[15, 16] stereocomplexation,[17-19] copolymerization[1, 20] and blending.[21, 22] While copolymers with P2HEB are rare,[14] PLA copolymers are now commonplace, with glycolide and ethylene glycol copolymers being the most commercially relevant.[23, 24] Many PLA copolymers seek to incorporate a more flexible comonomer, such as ε-caprolactone, which decreases crystallinity, T_g and T_m and increases the percentage strain at break of the copolymer.[25, 26] In comparison with the technical challenge of copolymerization, polymer blending is often a quick and cost-effective approach to upgrade the properties of individual polymer constituents. For example, poly(L-lactic acid) (PLLA) has been blended with many polymers including non-renewable polyolefins like poly(methyl methacrylate) (PMMA),[27] and other biodegradable systems such as poly(3-hydroxybutyrate-co-3-hydroxyvalerate) (PHBV)[28] and PCL.[29]

This paper explores the incorporation of the aromatic-aliphatic P2HEB polymer into PLLA through both blending of the two homopolymers over a range of compositions, and the preparation of diblock and triblock copolymers (Fig. 1). Full characterisation of the resulting thermal, optical and structural properties of the polyesters, along with their catalysed and enzymatic degradation, gives a complete picture of the impact of the process. The findings can shape the preparation of new recyclable plastics with enhanced properties.

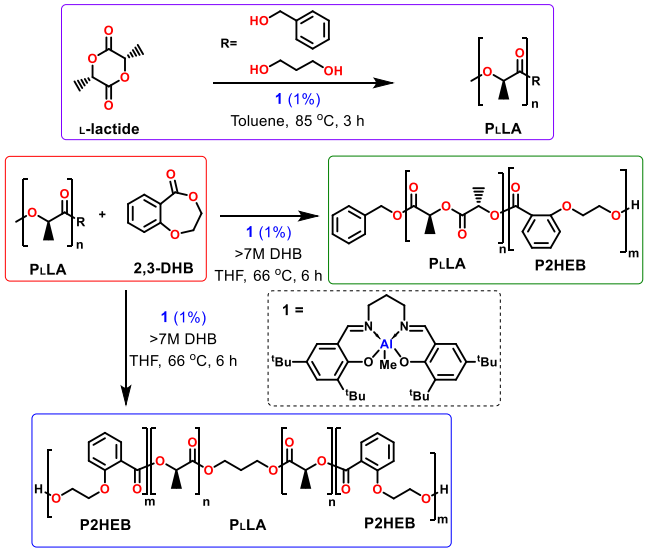

Figure 1. Ring opening polymerization of L-lactide and 2,3-DHB to form diblock and triblock copolymers using an aluminium salen catalyst.

2. Materials and Methods

2.1. Starting materials

Benzyl alcohol (BnOH) and 1,3-propanediol were dried for 24 hours under reflux with CaH_2 and then distilled under an inert atmosphere. Toluene and THF were collected from an Inert Atmospheres solvent purification system and degassed *via* three freeze–pump–thaw cycles prior to use. Chloroform (reagent grade ≥ 99.8%) was purchased from LabScan. 2,3-Dihydro-5H-1,4- benzodioxepin-5-one (2,3-DHB) was recrystallised three times from EtOAC : hexanes (50 : 50) prior to it being dried under vacuum and then sublimed.[14] L-Lactide was supplied by Corbion Ltd and purified by recrystallization from anhydrous toluene three times before sublimation. Aluminium salen **1** was synthesised following a published literature procedure.[30, 31] For the polymer blends, P2HEB with an M_n of 10.000 g mol^{-1} was

synthesised following published literature procedures,[13] while PLLA with an M_n of 100.000 g mol^{-1} was supplied by Purac Biochem.

2.2. Synthesis of BnOH-initiated PLLA

All synthetic procedures were conducted under an inert atmosphere using a Vigor glovebox equipped with a -35°C freezer and [H_2O] and [O_2] detectors. L-Lactide (2 g, 13.9 mmol), MeAl[salen] (108.4 mg, 0.2 mmol), and BnOH (20.6 µL, 0.2 mmol) were dissolved in toluene (13.8 mL) in an ampoule. The reaction was stirred for three hours at 85 °C prior to quenching with cold methanol followed by precipitation in cold methanol to afford the PLLA as a white solid (1.8 g), with spectroscopic data matching previously published work.

2.3. Synthesis of propanediol initiated homopolymer PLLA

L-Lactide (2.5 g, 17.3 mmol), MeAl[salen] (271.1 mg, 0.5 mmol), and 1,3 propanediol (17.8 µL, 0.25 mmol) were dissolved in toluene (17.4 mL) in an ampoule. The reaction was stirred for three hours at 85 °C prior to quenching with cold methanol followed by precipitation in cold methanol to afford the PLLA as a white solid (2.2 g), with spectroscopic data matching previously published work.

2.4. Synthesis of P2HEB-PLLA diblock copolymer

Homopolymer PLLA (0.3 g, 0.033 mmol), 2,3 DHB (0.38 g, 2.32 mmol), and MeAl[salen] (18.2 mg, 0.033 mmol) were dissolved in THF (0.3 mL) in an ampoule. The reaction was stirred for six hours at 66 °C prior to quenching with 10 % DCM in cold methanol followed by precipitation in cold methanol to afford the diblock copolymer as an off-white solid (1.2 g, Fig. 1). ^{1}H NMR (500 MHz, $CDCl_3$): δ 7.76 (t, 0.11H, Ar**H**), 7.38 (m, 0.11H ArH), 6.93 (m, 0.22H, Ar**H**), 5.16 (q, 1H, C(O)C**H**(CH_3)O), 4.57 (t, 0.22H, C(O)OC**H$_2$**CH_2O), 4.28 (t, 0.22H, C(O) OCH_2C**H$_2$**O). ^{13}C NMR (126 MHz, $CDCl_3$): δ 169.80 (**C**(O)CH(CH_3)O), 166.10 (**C**(O)OR), 158.56, 133.67, 131.87, 120.96, 120.81, 114.18 (Ar), 68.86 (C(O)**C**H(CH_3)O), 67.37 (C(O)OCH_2**C**H_2O), 62.97 (C(O)O**C**H_2CH_2O). 16.60 (C(O)CH(**C**H_3)O).

2.5. Synthesis of P2HEB-PLLA-P2HEB triblock copolymer

Diol homopolymer PLLA (1.4 g, 0.15 mmol), 2,3 DHB (1.7 g, 10.5 mmol), and MeAl[salen] (82.01 mg, 0.15 mmol) were dissolved in THF (0.3 mL) in an ampoule. The reaction was stirred for six hours at 66 °C prior to quenching with 10 % DCM in cold methanol followed by precipitation in cold methanol to afford the triblock copolymer as an off-white solid (1.2 g, Fig. 1). ^{1}H NMR (500 MHz, $CDCl_3$): δ 7.76 (m, 0.12H, Ar**H**), 7.38 (dd, 0.12H ArH), 6.93 (m, 0.29H, Ar**H**), 5.16 (q, 1H, C(O)C**H**(CH_3)O), 4.57 (m, 0.29H, C(O)OC**H$_2$**CH_2O), 4.28 (m, 0.29H, C(O) OCH_2C**H$_2$**O). ^{13}C NMR (126 MHz, $CDCl_3$): δ 169.80 (**C**(O)CH(CH_3)O), 166.10 (**C**(O)OR), 158.56, 133.67, 131.87, 120.96, 120.81, 114.18 (Ar), 68.86 (C(O)**C**H(CH_3)O), 67.37 (C(O)OCH_2**C**H_2O), 62.97 (C(O)O**C**H_2CH_2O). 16.60 (C(O)CH(**C**H_3)O).

2.6. Blend preparation

PLLA/P2HEB blends were prepared by a solvent-casting method. The requisite amount of each polymer to obtain 100/0, 80/20, 60/40, 50/50, 40/60, 20/80 and 0/100 compositions were dissolved in chloroform at a concentration of 10% (w/w) with vigorous magnetic stirring for 60 min. The resulting mixtures were cast onto a glass Petri dish and dried at 30 °C for 96 h in an oven. 150 µm thick films were obtained.

2.7. Characterization techniques

Gel permeation chromatography (GPC) was conducted on a Malvern Insturments Viscotek 270 GPC Max triple detection system with 2 mixed bed styrene/DVB columns (300 by 7.5 mm) in THF at a flow rate of 1 mL min^{-1} at 35 °C.

Proton Nuclear Magnetic Resonance (^{1}H-NMR) Spectroscopy was conducted in $CDCl_3$ on a Bruker Avance 500 MHz spectrometer.

The thermal behaviour of the copolymers and blends were determined using a Mettler Toledo differential scanning calorimetry (DSC) (DSC 822e) under nitrogen atmosphere (30 mL min^{-1}). Samples (8 ± 1 mg) were sealed in an aluminium pan, heated from -30 to 190 °C at a rate of 10 °C/min (termed as 1st heating) in order to determine thermal transitions (glass transition temperature (T_g), cold crystallization temperature (T_{cc}) and melting point temperature (T_m)) and held at 190 °C for 2 min to remove previous thermal history. Samples have been cooled to -30 °C and -50 °C (for the blends) at a rate of 50 °C/min and a subsequent heating scan at 10 °C/min was applied (termed as 2nd heating). Additionally, when cooling from 190 to -30 °C, two crystallization treatments were applied to the samples; non-isothermal crystallization by cooling the copolymers as 5 °C/min- and isothermal crystallization by holding the samples at T_c=80 for 200 min prior to cooling them to -30 °C.

Infrared spectra of blends were recorded on a Thermo Nicolet Nexus 670 Fourier transform infrared spectrophotometer (FTIR) using ATR mode. Each IR spectrum consisted of 32 scans taken in the range 400–4000 cm^{-1} with a resolution of 2 cm^{-1}. The average values over three replicates are reported.

Thermal degradation of copolymers and blends was studied using a Mettler Toledo 822e thermogravimetric analysis (TGA) in alumina pans with nitrogen flux of 50 mL min^{-1} for each sample (8 ± 1 mg). Samples were heated from room temperature to 500 °C at 2, 5, 10 and 20 °C/min and at 10 °C/min for the blends. Traces were normalized at 100 °C once the ~6% of the residual solvent arising from solvent-casting has been completely removed.

Ultraviolet–visible (UV-Vis) absorption spectra were recorded with a Shimadzu MultiSpec-1501 spectrophotometer. Total transmittance experiments have been analysed in the range of 190 to 800 nm with a

sampling interval of 1 nm and 25 accumulations. Approximately 150 µm thick films were obtained solvent-casting using dichloromethane. Morphology phase studies were performed in a Hitachi S-4800 field emission scanning electron microscope (FE-SEM) at an acceleration voltage of 5 kV. Before characterization, cryogenically fracture surfaces were gold-coated (15 nm thick layer) using an Emitech K550X sputter coater.

Surface topology of samples was analysed using a Dimension ICON atomic force microscope (AFM) from Bruker (Bruker Corporation, Coventry, UK). Experiments were carried out in tapping mode with an integrated silicon tip/cantilever.

Wide angle X-Ray diffraction (WAXD) patterns were measured using a Bruker D8 Advance diffractometer operating at 30 kV and 20 mA, equipped with a Cu tube (λ = 1.5418 Å), a Vantec-1 PSD detector, and an Anton Parr HTK2000 high-temperature furnace with a direct sample heating Pt sample holder. The powder patterns were recorded in 2θ steps of 0.033 ° in the $8 \leq 2\theta \leq 38$ range. The sample was measured through heating and cooling in the 30 – 250 °C range, each 5 °C at 10 °C/min.

Dynamic mechanical analyses (DMA) were performed on a DMA/SDTA861 analyser (Mettler-Toledo) in tensile mode. 150 µm thick samples of the copolymers (4 mm wide and 5.5 mm long) were obtained through solvent-casting method. Before characterization, dynamic strain sweep experiments over the 0.001–5 % range have been conducted to determine the linear viscoelastic region (LVR) of copolymers (Fig. S1). LVR has been determined as the onset of the storage modulus (E´) drop as a consequence of the sample overstrain. Curves displaying E´ and the energy loss (tan δ) were recorded as a function of temperature at a heating rate of 3 °C min^{-1}, a frequency of 1 Hz and displacement of 2 µm for the copolymers and 5 µm for the blends (to ensure that applied strain is within the LVR).

2.8. Degradation studies

Samples for degradation studies were prepared as follows. 0.55 g of the respective copolymers were dissolved in 6 mL of chloroform and pipetted, avoiding bubble deposition, onto a PTFE plate with a diameter of 7.8 mm. The PTFE plate was covered with a glass lid and placed on a balance to allow even evaporation of the solvent to form a film of 0.1 mm thickness.

Chemical degradation studies were carried out following a modified literature procedure,[13, 14] the respective polymers (0.0075 mmol) and MeAl[salen] (0.0045 mmol) were dissolved in THF (0.003 M) in an ampoule. The ampoule was heated to 70 °C for 20 hours. Product distributions were analysed by ^{1}H NMR spectroscopy.

Enzymatic degradation studies were done following a modified literature procedure,[32] the respective polymer films (cut to weigh a maximum of 12 mg) were placed in separate vials consisting of Tris-HCl buffer (5 mL, 50 mM, pH 8.6) and 1 mg of proteinase K. The vials were placed in an incubator at 37 °C on a rotary shaker set to 250 rpm. The study was carried out over 60 hours, analysing three separate replicates of each film every 12 hours. Analysis was carried out by removing the film from the buffer solution, rinsing it with distilled water and drying under vacuum (0.1 mmHg) at room temperature over phosphorus pentoxide until a constant mass was obtained. Product distributions were analysed by ^{1}H NMR spectroscopy.

3. Results and Discussion

3.1. Polymer synthesis

Aluminium salen catalysed ROP of L-lactide with either benzyl alcohol or 1,3 propanediol afforded the desired cores (Table 1, **1** and **2**, respectively) for diblock and triblock copolymers. The synthesised PLLA blocks were used as macroinitiators in the ROP of 2,3-DHB to afford the target copolymers **3** (diblock) and **4** (triblock). Maintaining a high concentration of DHB in solution was crucial to successful synthesis of **3** and **4** due to the precisely balanced monomer-polymer equilibrium, and thus very little solvent was used. THF was effective at dissolving the PLA macroinitiators at 66 °C, near the polymerization temperature of 2,3-DHB. The low conversions of 2,3-DHB to P2HEB observed were due to this monomer-polymer equilibrium and the maximum concentration that could be achieved whilst maintaining a homogenous solution. The dispersities of the diblock and triblock copolymers remained narrow (Table 1) and polymer composition was determined by ^{1}H NMR integration of the methine and aromatic resonances versus initiator resonances. Polymer **3** was composed of block lengths of 115:46 PLLA-P2HEB, while **4** had a composition of 15:100:15 with an expected even split suggested by the low Đ. Both the copolymers, and their blends with PLLA, were tested for their thermal and mechanical properties, as described below.

Table 1. Characterisation of PLLA cores and P2HEB-PLLA block copolymers.

Polymer	Conversion (%)	M_n (gmol^{-1})[f]	$M_{n,th}$ (gmol^{-1})[g]	Đ[f]
1[a]	95	9,498	10,196	1.05
2[b]	98	9,470	10,170	1.07
3[c]	20	16,932	21,687	1.15
4[d]	22	16,304	21,662	1.14

[a][l-lactide]$_0$:[Al]$_0$:[BnOH]$_0$=70:1:1; [b][l-lactide]$_0$:[Al]$_0$:[1,3-propanediol]$_0$=70:2:1; [c][2,3-DHB]$_0$:[Al]$_0$:[1]$_0$=70:1:1; [d][2,3-DHB]$_0$:[Al]$_0$:[2]$_0$= 70:1:1; [e]determined by ^{1}H NMR spectroscopy; [f]determined by triple-detection GPC, *dn/dc*=0.05; [g]$M_{n,th}$ = ([M]/[ini])×M_W(M)×(% conv.)+M_W(end group).

3.2. Thermal properties

The thermal transitions of the copolymers and the blends over a range of compositions were studied by DSC. During the first heating scan (Fig. 2a), the P2HEB-PLLA diblock copolymer undergoes a single heat enthalpy change centred at 15.2 °C, identified as the T_g. Increasing the temperature beyond the T_g led to a double endothermic event centred at 118.2 °C and 157.8 °C, associated with the double melting-behaviour of the P2HEB-PLLA copolymer. The P2HEB-PLLA-P2HEB triblock copolymer displays thermal transitions corresponding mainly to the larger portion of PLLA in the triblock copolymer. The triblock copolymer shows a T_g centred at 39.9 °C and a single T_m at 144.6 °C. The double-melting behaviour is difficult to discern due to an apparent overlap between the T_g of the copolymer and the T_m of short P2HEB blocks. The enthalpy of cold crystallization and fusion (ΔH_{cc} and ΔH_m respectively) determined as the area under the melting curve, was also calculated for both copolymers and is shown in Table S1. For both copolymers, upon crystallization at

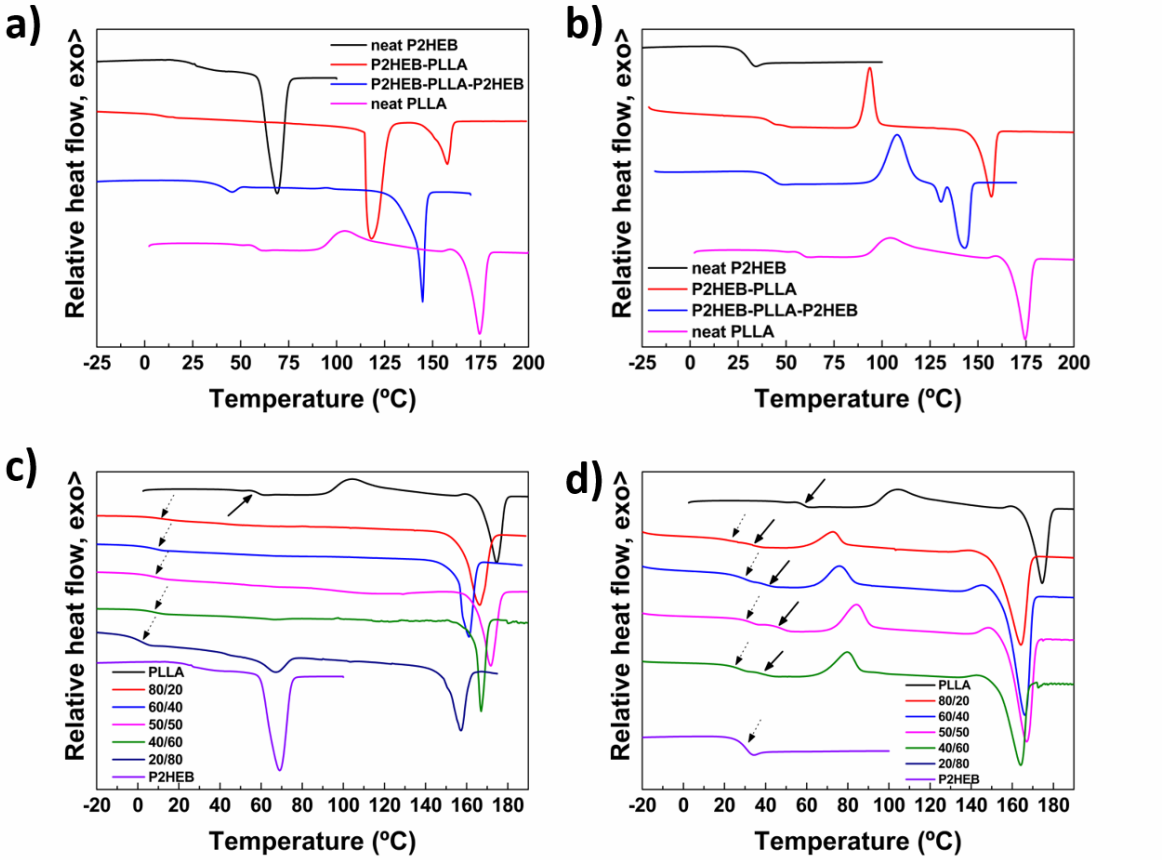

Figure 2. a) 1st and b) 2nd DSC heating traces of synthesized copolymers (traces corresponding to their homopolymers are also shown as a reference). c) 1st and d) 2nd DSC heating scans of PLLA/P2HEB blends (arrows indicate glass transition region for each blend constituent; dashed line for P2HEB).

temperatures between T_m and T_g (isothermally at 80 °C, Fig. S2, Table S1), only transitions corresponding to the PLLA block are observed, indicating that only the PLLA units recrystallise upon cooling. This is unsurprising due to the poor crystallizability of P2HEB which loses its nascent form upon melting.[13] Overall, the incorporation of P2HEB lowers the T_g and T_m of neat PLLA (55 and 175 °C respectively) up to an extent correlating with the proportion of P2HEB.

Beyond these block copolymers, the thermal transitions of the PLLA/P2HEB system was determined over the entire composition range after the preparation of 100/0, 80/20, 60/40, 50/50, 40/60, 20/80 and 0/100 blends. Miscible blends are known to display a single T_g located at temperatures intermediate between those of neat blend partners, while immiscible systems show two well-defined T_gs.[33-36] As shown in Fig. 2c and 2d, both blend constituents are semicrystalline, with a second order transition corresponding to the T_g followed by melting of crystalline domains at higher temperatures (see wide angle X-ray diffraction patterns, Fig. S3).[37, 38] As measured during the first DSC heating scan (Fig. 2c), neat PLLA displays a T_g at ~60 °C and a melting temperature (T_m) of 168 °C, while the T_g and T_m for the P2HEB are obtained at ~20 and ~70 °C respectively.[39, 40]

The specific heat change (ΔC_p) of PLLA, characteristic of its T_g, is rather weak because of the large crystalline fraction obtained during the solvent-casting method, which acts as a confining phase for the amorphous regions, reducing the molecular mobility of the system and thus decreasing the measured specific heat change.[40, 41] Despite the small ΔC_p observed for the PLLA fraction, all intermediate blends display a double T_g, in which the temperature remains in between the corresponding values of each individual counterparts, suggesting no interaction between partners, as reported for other polylactide-based systems.[42-45]

The second heating scan shown in Fig. 2d is obtained after the fast cooling (at -50 °C/min) from the melt of to remove the occluded chloroform and to obtain nearly amorphous samples. All the samples show a low temperature T_g and a melting event in the 150–165 °C range assigned ascribed to PLLA fraction (its height progressively decreases with the addition of P2HEB).[39]

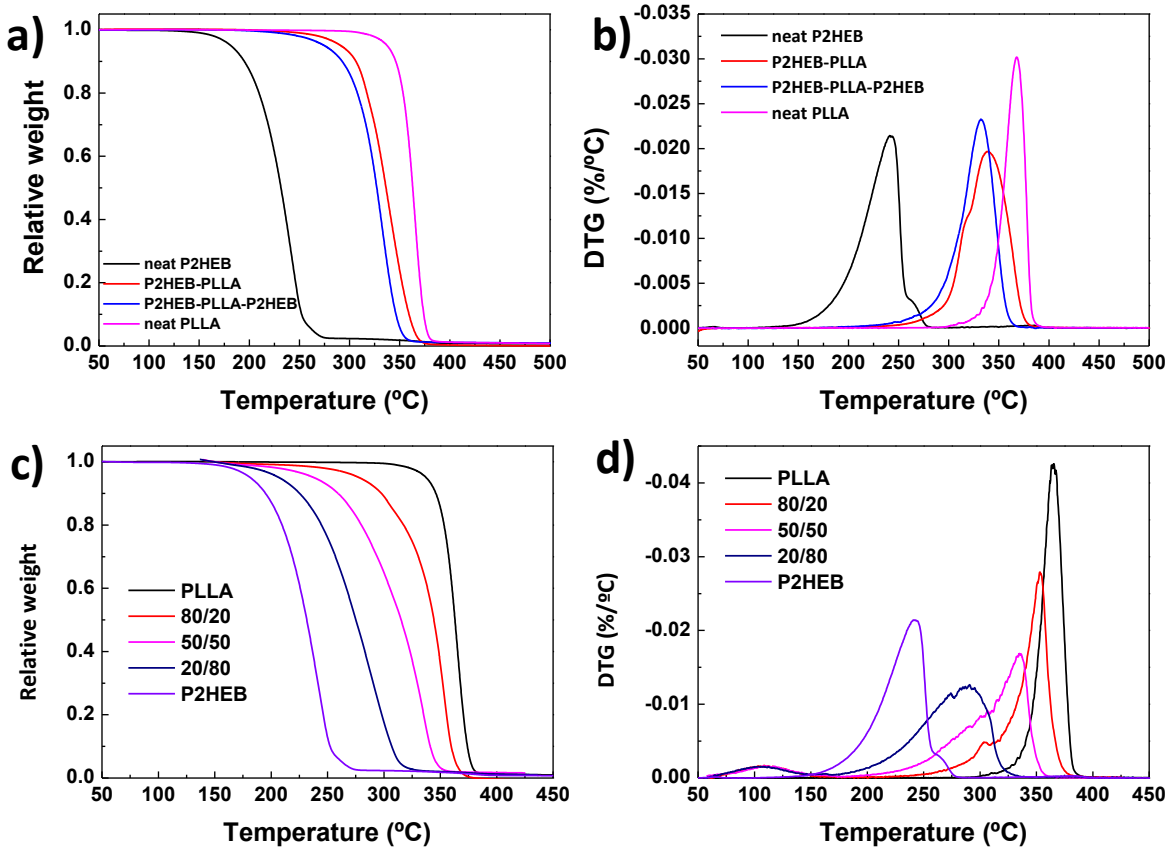

Figure 3. a) Thermogravimetric traces and b) weight lost rates (DTG) of copolymers and their homopolymers; c) thermogravimetric traces and d) weight lost rates (DTG) of PLLA/P2HEB blends.

The exothermic peak occurs because of cold-crystallization (T_{cc}) through the rearrangement of amorphous PLLA domains into new crystalline regions upon DSC heating. Therefore, the shifted T_gs of PLLA relative to Fig. 2a arises from its predominantly amorphous character after cooling from the melt. Both T_{cc} and T_m temperatures are decreased by ~15°C as P2HEB fraction increases indicating P2HEB may act as a nucleating agent whilst also preventing the development of thick lamellae, decreasing the T_m of PLLA.[15, 39, 40, 46] The full immiscibility of the PLLA/P2HEB system over the entire composition range observed through DSC was confirmed by Fourier transform infrared spectroscopy (FTIR) where the signal of the bands of the neat samples were almost unaltered after blending (Fig. S4).

Similar conclusions are obtained from DMA experiments (Fig. S5). Both the P2HEB-PLLA diblock and P2HEB-PLLA-P2HEB triblock copolymers present a glassy a region with rigid body behaviour where the storage modulus (E´) remains independent of the applied temperature. This modulus decrease is related to the sudden molecular mobility increase of chains, an α relaxation or T_g (T_gs of 39.4 and 25.7 °C for the diblock and triblock respectively are obtained, which agree well with DSC values). Contrarily, two well-defined α relaxation processes at ~28 and 62 °C are observed from blends, supporting immiscibility. The incorporation of P2HEB also increases the strain at break of the copolymer compared to neat PLLA.

Thermogravimetric analysis (TGA) was performed to determine the thermal stability of synthesized copolymers and blends. Fig. 3a and 3b display the thermogravimetric traces and weight lost rates (DTG) of the copolymers and their homopolymers, with parameters listed in Table S2. Copolymerization with PLLA gives P2HEB-based materials with a marked increased thermal stability with respect to its homopolymer, with the onset of thermal degradation ($T_{5\%}$) increasing by over 110 °C. As shown in the first derivative of weight loss against temperature curves (DTG, Fig. 3b), an increase in the number of PLLA repeat units led to an increase in the maximum degradation rate temperature (T_{peak}), as a consequence of the higher thermal stability of PLLA (see Fig. S6 for heating rate effects). Single peak degradation for both homopolymers is observed. Conversely, the copolymers exhibit small shoulders corresponding to P2HEB degradation temperatures, suggesting degradation of the less thermally stable P2HEB sequences. Interestingly, both DTG peaks remain almost completely overlapped in these copolymers, although the DTG curves of each homopolymer differ by 130 °C,[13, 16] which may arise from a randomised thermally-induced disintegration.[47] Indeed, the two thermodegradation events are more overlapped in the P2HEB-PLLA-P2HEB triblock as the sequences are more intercalated between P2HEB, decreasing its thermal stability. These results highlight the potential of copolymerization to upgrade the poor thermal stability of P2HEB.

Thermogravimetric traces (Fig. 3c) and weight loss rates (Fig. 3d) of the blends indicate that the blends thermally degrade in two main stages, with thermodegradation of P2HEB followed by the more thermally stable PLLA phase, resulting in a full width at half maximum (FWHM) of blends larger than that of pure counterparts. For instance, the FWHM of PLLA and P2HEB are 21 and 49 °C respectively, while 20/80 blend presents a FWHM of 59 °C, indicating a more complex degradation mechanism when both partners are blended.

3.3. Optical properties

The optical properties of bioplastics are often a drawback that limits prospective applications, such as in packaging. Poly(lactic acid)s are highly permeable to UV light,[48, 49] impacting food quality and shelf life.[50] A plausible approach to prevent food photodegradation would be to develop biopolymers with UV-light barrier properties comparable to poly(ethylene terephthalate) (PET). While dispersed nanofillers, polymer blends, or UV-absorbing compounds have been previously explored,[16, 51] we hypothesized that copolymerization of PLA with the UV-absorbing P2HEB may improve the polymer performance, whilst avoiding the challenges of nanocomposite processing and the incompatibility of blending. The UV-Vis transmittance of the P2HEB-PLLA diblock and P2HEB-PLLA-P2HEB triblock copolymers are shown in Fig. 4. Homopolymer PLLA transmits almost 100 % of the light in the 250-800 nm region, with a transparency (determined as the transmission of light from 540–560 nm; ASTM D1746-03) of 97.6 %.[52] On the contrary, neat P2HEB is a strong UV absorber, blocking both UV-B light (λ=280-315 nm) and UV-A light (λ=315-400 nm).[53] The maximum absorption wavelength (λ_{max} = 333 nm) matches that of other aromatic-containing polymers such as poly(4-(2-thiophenyl)styrene) (PTS) or poly(5- hexyl-5´´-(4-vinylphenyl)-2,2´:5´,2´´-terthiophene) (PH3TS).[54] As a homopolymer, however, its low visible transparency (60.2 %) limits its use in transparent packaging. For the di- and tri-block copolymers, excellent combined properties result, showing both UV-blocking and optical transparency. More precisely, these copolymers block close to 100 % of UV-B light while maintaining an optical transparency of 75 %, offering a sustainable alternative to common copolymers such as PS-b-PMMA.[55] This suggests strong potential in packaging applications, especially for the P2HEB-PLLA-P2HEB triblock. Note that this good transparency suggest that copolymers do not show separated domains larger than the wavelength of light studied (*vide infra*).[56]

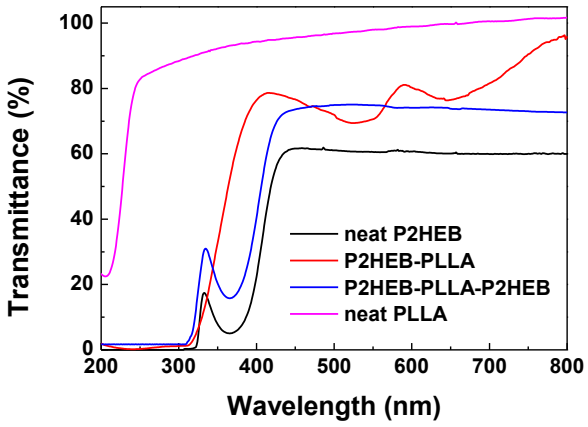

Figure 4. UV-Vis transmittance spectra for neat P2HEB, neat PLA and the diblock P2HEB-PLLA and P2HEB-PLLA-P2HEB triblock copolymers.

3.4. Morphology

As the copolymers are formed of chemically distinct, covalently bound, blocks,[13] phase- or microphase-separated morphologies may result from their self-assembly into well-defined domains.[57] Scanning electron microscopy (SEM) was thus used to investigate the morphology of the block copolymers and blends (Fig. S7). Both diblock and triblock copolymers show a single phase over the analysed length scale. On the contrary, PLLA/P2HEB blends, exhibit a strong phase separation (even in the presence of the copolymer as a compatibiliser) characterized by a two-phase sea-island morphology with aggregates of about 5-12 μm similarly to other PLA-based immiscible blends with poly(N-isopropylacrylamide),[58] poly[(butylene succinate)-co-adipate],[59] PCL,[60] or poly(ethylene-co-vinyl acetate).[61] The absence of macrophase separation for the copolymers is ascribed to a strong interaction between P2HEB and PLLA phases.

Since phase separation could also occur at a smaller scale forming lamellar, cylindrical and spherical features,[57] atomic force microscopy (AFM) was used to explore if there is any phase-separation at the nanoscale level. As shown in Fig. 5, experiments were carried out at two different temperatures to better understand how thermal transitions affect their nanoscale morphology. AFM height and phase images are shown on the left and right part of each box respectively. In the height image bright and dark regions correspond to mountains and valleys respectively,
while in the phase image the bright regions are indicative of the hard phase material.[62] It is observed that, at room temperature both copolymers display a characteristic microphase separation with domain sizes between 40-200 nm.[63] Phase image reveals that the soft segment remains dispersed within the hard continuous phase. Since at room temperature P2HEB presents a lower modulus than PLLA,[13] such dark areas are identified as P2HEB phase. As temperature is increased to 150 °C, copolymers are able to recrystallize and the PLLA fraction forms well-defined 15 nm thick lamellae which are surrounded by amorphous yet soft P2HEB regions (dark regions). These novel forming crystalline domains have been also observed in the form of an exothermic crystallization peak during the DSC heating scans in Fig. 2.

3.5. Crystalline structure studies

Wide angle X-Ray diffraction (WAXD) was used to confirm that the fraction that crystallised within the copolymers corresponds only to PLLA sequences. Fig. 6a shows the X-ray diffraction patterns of the P2HEB-PLLA diblock and P2HEB-PLLA-P2HEB triblock copolymers. Both copolymers only display the featured reflections corresponding to the 10_3 helical conformation of PLLA α crystal form at 2θ values of 14.8, 16.5, 19.0 and 22.3° attributed to *(010)*, *(110)/(200)*, *(203)* and *(015)* planes, respectively.[64, 65] This proves that only the PLLA fraction is able to crystallise in the copolymers, similar to what was found in a different copolyester, poly(ω-PDL-co-d-HL).[47] High temperature X-ray

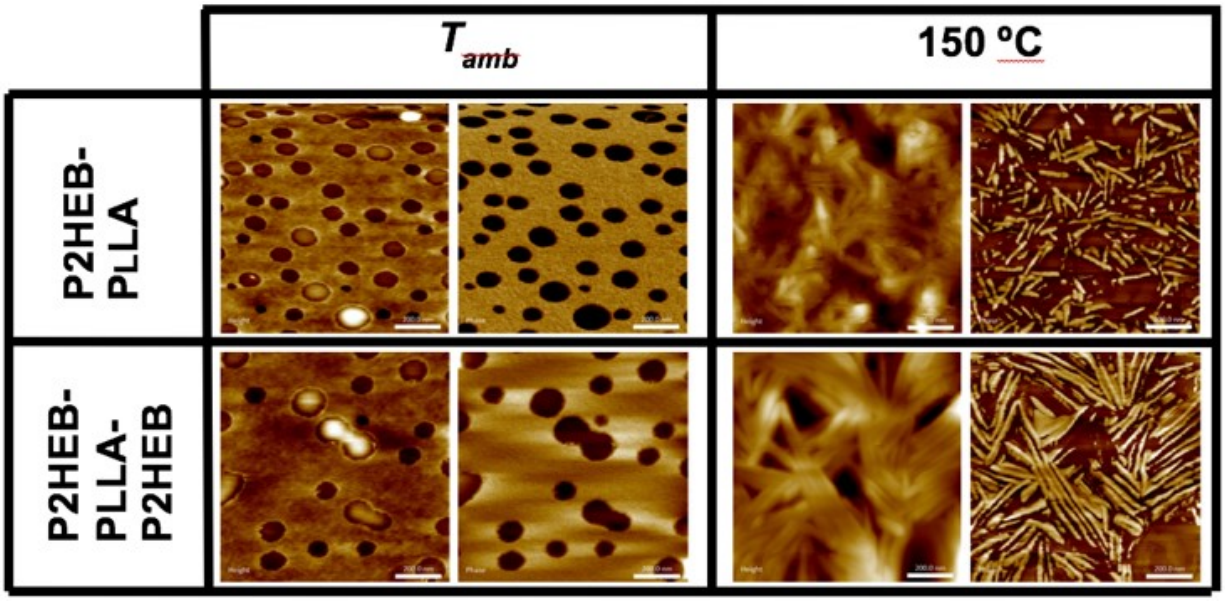

Figure 5. AFM height and phase images (left and right images in each box respectively) of the P2HEB-PLLA diblock and P2HEB-PLLA-P2HEB triblock copolymers at room temperature and 150 °C. Each scale bar represents 200 nm.

patterns were further recorded from room temperature up to 250 °C, where after extracting the background, the intensity area of the most relevant *(110)* maxima of the copolymers was calculated (Fig. 6b). All the crystal reflection intensity disappears once the melting temperature of PLLA crystals is reached (at 160 and 145 °C for P2HEB-PLLA and P2HEB-PLLA-P2HEB copolymers respectively). In the other hand, no significant changes in the diffraction patterns are observed in the temperature range at which P2HEB crystals melt, which has been reported to occur in the 68.8 - 76.8 °C temperature range for P2HEB having 11.600 and 40.300 g mol^{-1} respectively.[13] In the light of these results and together with DSC data we reinforce our hypothesis that only PLLA phase of the copolymers is able to crystallise.

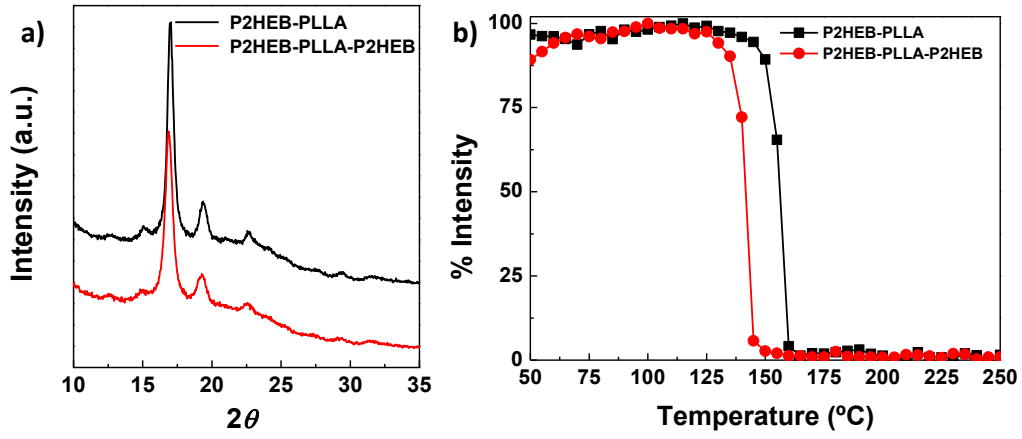

Figure 6. a) 2D-WAXD diffractograms obtained for the diblock and triblock copolymers at room temperature and b) evolution behaviour for the X-ray diffraction intensity area of the *(110)* reflection for the diblock and triblock copolymers upon increasing temperature.

3.6. Block copolymer degradation

One of the intriguing properties of the aliphatic-aromatic polymer P2HEB is its selective chemical degradation depending upon a finely balanced monomer-polymer equilibrium. Both homopolymers of 2,3-DHB and copolymers with a highly ring-strained comonomer, β-butyrolactone,[14] showed selective degradation to monomer, with >80% degradation to cyclic monomer in 1 h. However, depolymerization of polymers **3** and **4** is complicated by the ready transesterification of the PLA block. Thus, both enzymatic and chemical degradation of the block copolymers was pursued.

Enzymatic degradation studies were carried out on the polymer films of the diblock and triblock copolymers. The polymer films were solution cast from chloroform to afford 100 µm thick films. Films were cut into 12 mg segments and exposed to proteinase K in a tris-HCl buffer for 60 hours, monitoring the degree of degradation every 12 hours by GPC vs. polystyrene standards (Fig. 7). Previous studies have shown that enzymatic degradation of PLLA favours the amorphous region of the polymer matrix, and is best for low molecular weight PLLA, with high surface areas.[32, 66] Interestingly, diblock copolymer, **3**, gave rise to a bimodal GPC trace upon enzymatic degradation. The higher hydrodynamic volume fraction decreased in weight fraction over time, with a low hydrodynamic volume fraction (3300 g mol^{-1}) increased. This may be due to the selective degradation of the non-crystalline P2HEB blocks, affording short, broad dispersity, PLLA segments.

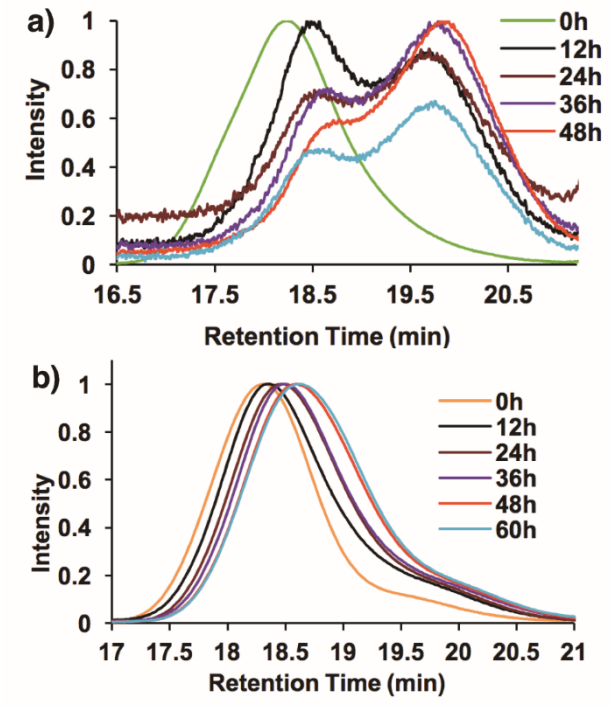

Figure 7. GPC traces of a) diblock 3 and b) triblock 4 copolymers measured vs. polystyrene standards.

Diffusion Ordered Spectroscopy (DOSY) was carried out to gain structural information on the degraded polymers (Fig. S8). While initial samples showed clear formation of copolymers, diffusing together, samples of the diblock (and indeed the triblock) showed that P2HEB and PLLA resonances correlated with different diffusion constants. Additionally, in the diblock copolymer, the P2HEB was indeed absent from NMR spectra, suggesting fast degradation of this block. In the triblock system, spectra suggested that degradation occurs by a more random chain scission. This observation correlates well with the more regular enzymatic degradation of triblock copolymer **4** (Fig. 8b), with slow but steady degradation of 23% degradation over 60 hours.

In each case, the enzymatic degradation is slower than that of the parent homopolymers.[13, 67] The copolymers show a sharp XRD peak at 17°, along with a small broader peak, suggesting some long range ordering. This high crystallinity may be contributing to this slower degradation, with more difficult access to the amorphous regions. While the aromatic rings in P2HEB orient to block order and crystallinity, they can also facilitate crystallinity in the PLLA blocks and may further reduce enzyme access for steric reasons. This reduction in enzymatic degradation rates has been previously observed in PCL-PLLA copolymers.[66]

Chemical degradation of the P2HEB-PLLA diblock and P2HEB-PLLA-P2HEB triblock copolymers were attempted under the same conditions as previously published for homopolymers, catalysed by the aforementioned aluminium salen catalyst, however THF was used due to the insolubility of the polymers in toluene at 70 °C; as this is a coordinating solvent, chemical degradation rates are expected to be lower. The quantity of solvent used also plays a key role in the extent and rate of degradation due to the monomer-polymer equilibrium. Dilute conditions were required to shift the monomer-polymer equilibrium to monomer. ^{1}H NMR spectroscopy was used to determine the percentage of degradation by relative integration of monomer and polymer peaks (Fig. 8). Depolymerization of the P2HEB blocks competes with the intramolecular transesterification of the PLLA in both copolymers. At these low catalyst loadings (0.0045 mmol [Al]), the diblock showed a maximum 29% depolymerization of the P2HEB block back to its cyclic monomer, 2,3-DHB. Interestingly, 6.7% of the PLLA block also degraded to the lactide monomer. This trend was also observed for the triblock with 26 and 5% depolymerization of P2HEB and PLLA respectively. With no further degradation observed beyond the initial 5h (Fig. S9), an increased extent of degradation was sought by increasing the catalyst concentration tenfold (Fig. 8). With 53% and 34% depolymerization of P2HEB and PLA blocks for diblock **3** and 89% and 60% depolymerization

of P2HEB and PLLA for triblock **4**, catalyst loading played a significant role in the extent of degradation.

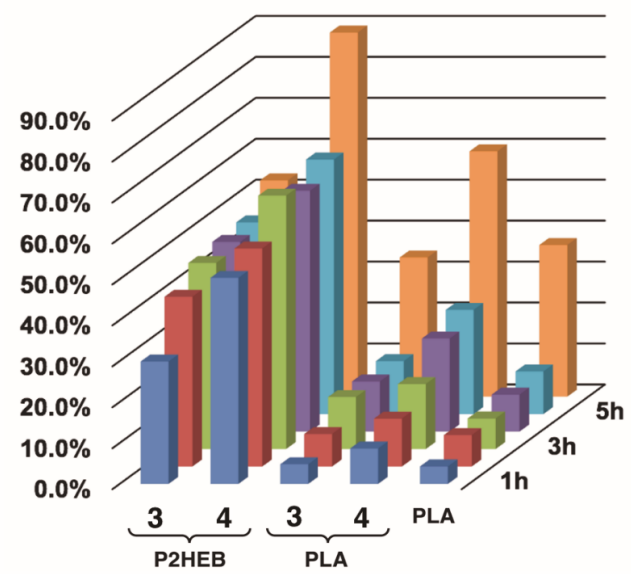

Figure 8. Percentage degradation determined by ^{1}H NMR over a 20 hour period for the P2HEB-PLLA diblock and P2HEB-PLLA-P2HEB triblock copolymer with 0.045 mmol of the aluminium salen catalyst.

It is clear that the transesterification of the lactide block significantly compromises the selectivity of the degradation of the P2HEB polymer. Indeed, diblock **3** behaves very similarly to that of isotactic PLLA. The faster transesterification of the lactic acid units dominates the chemical degradation, preventing clean and selective block depolymerization as previously observed. Interestingly, the triblock copolymer **4** actually promotes lactide formation, suggesting that other copolymer formulations may lead to alternative chemical recycling strategies.

4. Conclusion

The controlled synthesis of the P2HEB-co-PLLA diblock and triblock copolymers was achieved through the sequential ring-opening polymerization of lactide and 2,3-DHB monomers with mono- and bi-functional initiators, while complementary polymer blends were prepared through solvent-casting. The thermal properties of P2HEB were modulated by the addition of the PLA comonomer, with an increase in thermal transition and stability temperatures. The blends conversely showed no interaction, with two T_gs and a two-step degradation is observed. The optical properties of the copolymers were studied due to the limitations of PLLA in absorbing UV light. The copolymers provided a significant advantage for potential packaging applications, with nearly 100% UV-B blocking and optical transparencies up to 75%. Large scale phase separation coupled with two α relaxation processes confirmed the non-interaction of the two polymers has been observed for the blends. Conversely, the copolymers showed phase separation only at the nanoscale. Both enzymatic and chemical degradation of the copolymers were slower than that of their respective homopolymers, with competing transesterification complicating the selective depolymerization of P2HEB blocks. The study showcases the importance of forming copolymers in modulating polymer properties over simple blends, and opens up new avenues for potential exploitation of the unique 2,3-DHB monomer.

Acknowledgments

The authors would like to thank the University of Edinburgh and the EPSRC for support through the Soft Matter and Functional Interfaces Centre for Doctoral Training (Grant Ref. No. EP/L015536/1) and the Marie-Curie Actions Programme (Grant FP7-PEOPLE-2013-CIG-618372). The authors also thank the Basque Country Government for financial support (IT718-13). Technical and human support provided by SGIker (UPV/EHU, MICINN, GV/EJ, EGEF and ESF) is gratefully acknowledged. The authors would finally like to thank Corbion Ltd. for the supply of L-lactide.

References

1. Gross, R. A. & Kalra, B. (2002) Biodegradable polymers for the environment. *Science* **297(5582)**:803-807.
2. Ulery, B. D., Nair, L. S. & Laurencin, C. T. (2011) Biomedical Applications of Biodegradable Polymers. *Journal of Polymer Science Part B-Polymer Physics* **49(12)**:832-864.
3. Scott, G. (2005) *Biodegradable Polymers for Industrial Applications.* 1st edn., Elsevier.
4. Seyednejad, H., Ghassemi, A. H., Van Nostrum, C. F., Vermonden, T. & Hennink, W. E. (2011) Functional aliphatic polyesters for biomedical and pharmaceutical applications. *Journal of Controlled Release* **152(1)**:168-176.
5. Ikada, Y. & Tsuji, H. (2000) Biodegradable polyesters for medical and ecological applications. *Macromolecular Rapid Communications* **21(3)**:117-132.
6. Hoskins, J. N. & Grayson, S. M. (2011) Cyclic polyesters: synthetic approaches and potential applications. *Polymer Chemistry* **2(2)**:289-299.
7. Kricheldorf, H. R. (2001) Syntheses and application of polylactides. *Chemosphere* **43(1)**:49-54.
8. Sinclair, F., Chen, L., Greenland, B. W. & Shaver, M. P. (2016) Installing Multiple Functional Groups on Biodegradable Polyesters via Post-Polymerization Olefin Cross-Metathesis. *Macromolecules* **49(18)**:6826-6834.
9. Jamshidian, M., Tehrany, E. A., Imran, M., Jacquot, M. & Desobry, S. (2010) Poly-Lactic Acid: Production, Applications, Nanocomposites, and Release Studies. *Comprehensive Reviews in Food Science and Food Safety* **9(5)**:552-571.
10. Hoglund, Anders, Karin, O. & Christine, A. A. (2012) Crucial differences in the hydrolytic degradation between industrial polylactide and laboratory-scale poly(L -lactide). *ACS Applied Materials and Interfaces* **4(5)**:2788-2793.
11. Hoglund, Anders, Minna, H., Ulrica, E. & Christine, A. A. (2010) Surface modification changes the degradation process

and degradation product pattern of polylactide. *Langmuir* **26(1)**:378-383.
12. Hong, M. & Chen, E. Y. X. (2017) Chemically recyclable polymers: a circular economy approach to sustainability. *Green Chemistry* **19(16)**:3692-3706.
13. Lizundia, E., Makwana, V. A., Larraaga, A., Vilas, J. L. & Shaver, M. P. (2017a) Thermal, structural and degradation properties of an aromatic–aliphatic polyester built through ring-opening polymerisation. *Polymer Chemistry* **8**:3530-3538.
14. Macdonald, J. P. & Shaver, M. P. (2016) An aromatic/aliphatic polyester prepared via ring-opening polymerisation and its remarkably selective and cyclable depolymerisation to monomer. *Polymer Chemistry* **7(3)**:553-559.
15. Lizundia, E., Vilas, J. L. & León, L. M. (2015) Crystallization, structural relaxation and thermal degradation in Poly(L-lactide)/cellulose nanocrystal renewable nanocomposites. *Carbohydrate Polymers* **123**:256-265.
16. Lizundia, E., Vilas, J. L., Sangroniz, A. & Etxeberria, A. (2017) Light and gas barrier properties of PLLA/metallic nanoparticles composite films. *European Polymer Journal* **91**:10-20.
17. Ahmed, J., Varshney, S. K. & Janvier, F. (2014) Rheological and thermal properties of stereocomplexed polylactide films. *Journal of Thermal Analysis and Calorimetry* **115(3)**:2053-2061.
18. Dai, J., Bai, H., Liu, Z., Chen, L., Zhang, Q. & Fu, Q. (2016) Stereocomplex crystallites induce simultaneous enhancement in impact toughness and heat resistance of injection-molded polylactide/polyurethane blends. *RSC Advances* **6(21)**:17008-17015.
19. Pound-Lana, G., Rabanel, J.-M., Hildgen, P. & Mosqueira, V. C. F. (2017) Functional polylactide via ring-opening copolymerisation with allyl, benzyl and propargyl glycidyl ethers. *European Polymer Journal* **90**:344-353.
20. Sabbatier, G., Larraaga, A., Guay- B, G. A. E. A., Fernandez, J., Di Val, F., Durand, B., Sarasua, J. R. & Laroche, G. T. (2015) Design, Degradation Mechanism and Long-Term Cytotoxicity of Poly(l -lactide) and Poly(Lactide-co-epsilon-Caprolactone) Terpolymer Film and Air-Spun Nanofiber Scaffold. *Macromolecular Bioscience* **15(10)**:1392-1410.
21. Harada, M., Iida, K., Okamoto, K., Hayashi, H. & Hirano, K. (2008) Reactive compatibilization of biodegradable poly(lactic acid)/poly(epsilon-caprolactone) blends with reactive processing agents. *Polymer Engineering and Science* **48(7)**:1359-1368.
22. Lu, X., Zhao, J. Q., Yang, X. Y. & Xiao, P. (2017) Morphology and properties of biodegradable poly (lactic acid)/poly (butylene adipate-co-terephthalate) blends with different viscosity ratio. *Polymer Testing* **60**:58-67.
23. Athanasiou, K. A., Agrawal, C. M., Barber, F. A. & Burkhart, S. S. (1998) Orthopaedic applications for PLA-PGA biodegradable polymers. *Arthroscopy* **14(7)**:726-737.
24. Du, Y. J., Lemstra, P. J., Nijenhuis, A. J., Vanaert, H. A. M. & Bastiaansen, C. (1995) ABA type copolymers of lactide with poly(ethylene glycol)-kinetic, mechanistic, and model studies. *Macromolecules* **28(7)**:2124-2132.
25. Jeon, O., Lee, S. H., Kim, S. H., Lee, Y. M. & Kim, Y. H. (2003) Synthesis and characterization of poly(L-lactide)-poly(epsilon-caprolactone) multiblock copolymers. *Macromolecules* **36(15)**:5585-5592.
26. Zhang, C. M., Zhai, T. L., Turng, L. S. & Dan, Y. (2015) Morphological, Mechanical, and Crystallization Behavior of Polylactide/Polycaprolactone Blends Compatibilized by L-Lactide/Caprolactone Copolymer. *Industrial & Engineering Chemistry Research* **54(38)**:9505-9511.
27. Hao, X., Kaschta, J., Pan, Y., Liu, X. & Schubert, D. W. (2016) Intermolecular cooperativity and entanglement network in a miscible PLA/PMMA blend in the presence of nanosilica. *Polymer* **82**:57-65.
28. Dasan, Y. K., Bhat, A. H. & Ahmad, F. (2017) Polymer blend of PLA/PHBV based bionanocomposites reinforced with nanocrystalline cellulose for potential application as packaging material. *Carbohydrate Polymers* **157**:1323-1332.
29. Davachi, S. M. (2017) Interface modified polylactic acid/starch/poly (epsilon-caprolactone) antibacterial nanocomposite blends for medical applications. *Carbohydrate Polymers* **155**:336-344.
30. Berry, M. T., Castrejon, D. & Hein, J. E. (2014). Oxidative Esterification of Aldehydes Using Mesoionic 1,2,3-Triazolyl Carbene Organocatalysts. *Org. Lett* . **16**:3676-3679.
31. Atwood, D. A., Hill, M. S., Jegier, J. A. & Rutherford, D. (1997). The Use of Five-Coordinate Aluminum Alkyls To Prepare Molecules Containing a Single Al− O− Si Linkage. *Organometallics* **16**:2659-2664.
32. Ohkita, T. & Lee, S. H. (2006) Thermal degradation and biodegradability of poly (lactic acid)/corn starch biocomposites. *Journal of Applied Polymer Science* **100(4)**:3009-3017.
33. Wang, H., Yang, P., Zhu, R. & Gu, Y. (2016) Preparation and characterization of novel multi-branched polymers in situ cured from benzoxazine/epoxy resin/primary amines blends. *RSC Advances* **6(18)**:15271-15278.
34. Aydin, A. A. & Ilberg, V. (2016) Effect of different polyol-based plasticizers on thermal properties of polyvinyl alcohol:starch blends. *Carbohydrate Polymers* **136**:441-448.
35. Lizundia, E., Gmez-Galvn, F., Prez, L., Len Alvarez, L. M. & Vilas, J. L. (2016) Poly(L-lactide)/branched Beta-cyclodextrin blends: thermal, morphological and mechanical properties. *Carbohydrate Polymers* **144**:25-32.
36. Morro, A., Catalina, F., Corrales, T., Pablos, J. L., Marin, I. & Abrusci, C. (2016) New blends of ethylene-butyl acrylate copolymers with thermoplastic starch. Characterization and bacterial biodegradation. *Carbohydrate Polymers* **149**:68-76.
37. Kalb, B. & Pennings, A. J. (1980) General crystallization behaviour of poly(l-lactic acid). *Polymer* **21(6)**:607-612.
38. Wunderlich, B. (2003) Reversible crystallization and the rigid-amorphous phase in semicrystalline macromolecules. *Progress in Polymer Science (Oxford)* **28(3)**:383-450.
39. Lizundia, E., Oleaga, A., Salazar, A. & Sarasua, J. R. (2012) Nano- and microstructural effects on thermal properties of poly (l-lactide)/multi-wall carbon nanotube composites. *Polymer* **53**:2412-2421.
40. Lizundia, E., Petisco, S. & Sarasua, J.R. (2012b) Phase-structure and mechanical properties of isothermally melt-and cold-crystallized poly (L-lactide). *Journal of the Mechanical Behavior of Biomedical Materials* **17**:242-251.
41. Pyda, M., Bopp, R. C. & Wunderlich, B. (2004) Heat capacity of poly(lactic acid). *Journal of Chemical Thermodynamics* **36(9)**:731-742.
42. Gardella, L., Calabrese, M. & Monticelli, O. (2014) PLA maleation: an easy and effective method to modify the properties of PLA/PCL immiscible blends. *Colloid and Polymer Science* **292(9)**:2391-2398.
43. Arias, V., Hglund, A., Odelius, K. & Albertsson, A.-C. (2014) Tuning the Degradation Profiles of Poly(l-lactide)-Based

Materials through Miscibility. *Biomacromolecules* **15(1)**:391-402.
44. Liu, Q., Wu, C., Zhang, H. & Deng, B. (2015) Blends of polylactide and poly(3-hydroxybutyrate-co-3-hydroxyvalerate) with low content of hydroxyvalerate unit: Morphology, structure, and property. *Journal of Applied Polymer Science* **132(42)**.
45. Lv, Q., Wu, D., Xie, H., Peng, S., Chen, Y. & Xu, C. (2016) Crystallization of poly(epsilon-caprolactone) in its immiscible blend with polylactide: insight into the role of annealing histories. *RSC Advances* **6(44)**:37721-37730.
46. Tsuji, H., Tezuka, Y., Saha, S. K., Suzuki, M. & Itsuno, S. (2005) Spherulite growth of l-lactide copolymers: Effects of tacticity and comonomers. *Polymer* **46(13)**:4917-4927.
47. Fernandez, J., Etxeberria, A. & Sarasua, J.R. (2016) Synthesis and properties of small omega -pentadecalactone-co- small delta -hexalactone copolymers: a biodegradable thermoplastic elastomer as an alternative to poly(epsilon-caprolactone). *RSC Advances* **6(4)**:3137-3149.
48. Auras, R., Harte, B. & Selke, S. (2004) An overview of polylactides as packaging materials. *Macromolecular Bioscience* **4(9)**:835-864.
49. Lizundia, E., Ruiz-Rubio, R., Vilas, J. L., & León, L. M. (2016) Poly(L-lactide)/ZnO nanocomposites as efficient UV-shielding coatings for packaging applications. *Journal of Applied Polymer Science* **132**:42426.
50. Turhan, K. N. & Sahbaz, F. (2001) A simple method for determining light transmittance of polymer films used for packaging foods. *Polymer International* **50(10)**:1138-1142.
51. Narayanan, M., Loganathan, S., Valapa, R. B., Thomas, S. & Varghese, T. O. (2017) UV protective poly(lactic acid)/rosin films for sustainable packaging. *International Journal of Biological Macromolecules* **99**:37-45.
52. Auras , R. A., Lim, L.-T., Selke, S. E. M. & Tsuji, H. (2010) *Poly(lactic acid): Synthesis, Structures, Properties, Processing, and Applications.*
53. Li, Y.Q., Fu, S.Y. & Mai, Y.-W. (2006) Preparation and characterization of transparent ZnO/epoxy nanocomposites with high-UV shielding efficiency. *Polymer* **47(6)**:2127-2132.
54. Hu, Z. & Reichmanis, E. (2011) Synthesis of electroactive polystyrene derivatives para-substituted with conjugated oligothiophene via postgrafting functionalization. *Journal of Polymer Science, Part A: Polymer Chemistry* **49(5)**:1155-1162.
55. Cano, L. (2014) Optical and Conductive Properties of As-Synthesized Organic-Capped TiO2 Nanorods Highly Dispersible in Polystyrene-block-poly(methyl methacrylate) Diblock Copolymer. *ACS Applied Materials & Interfaces* **6(14)**:11805-11814.
56. Gutierrez, J., Carrasco-Hernandez, S., Barud, H. S., Oliveira, R. L., Carvalho, R. A., Amaral, A. C. & Tercjak, A. (2017) Transparent nanostructured cellulose acetate films based on the self assembly of PEO-b-PPO-b-PEO block copolymer. *Carbohydrate Polymers* **165**:437-443.
57. Kim, H.-C., Park, S.-M. & Hinsberg, W. D. (2010) Block Copolymer Based Nanostructures: Materials, Processes, and Applications to Electronics. *Chemical Reviews (Washington, DC, United States)* **110(1)**:146-177.
58. Lizundia, E., Meaurio, E., Laza, J. M. & Vilas, J. L. (2015) Study of the chain microstructure effects on the resulting thermal properties of poly(L-lactide)/poly(N-isopropylacrylamide) biomedical materials. *Materials Science & Engineering C* **50**:97-106.
59. Ojijo, V. (2012) Role of Specific Interfacial Area in Controlling Properties of Immiscible Blends of Biodegradable Polylactide and Poly (butylene succinate)-co-adipate. *ACS Applied Materials & Interfaces* **4(12)**:6690-6701.
60. Rizzuto, M., Mugica, A., Zubitur, M., Caretti, D. & Muller, A. J. (2016) Plasticization and anti-plasticization effects caused by poly(lactide-ran-caprolactone) addition to double crystalline poly(l-lactide)/poly(epsilon-caprolactone) blends. *Crystal English Communication* **18(11)**:2014-2023.
61. Li, Y., Liu, L., Shi, Y., Xiang, F., Huang, T., Wang, Y. & Zhou, Z. (2011) Morphology, rheological, crystallization behavior, and mechanical properties of poly(L -lactide)/ethylene-co-vinyl acetate blends with different VA contents. *Journal of Applied Polymer Science* **121(5)**:2688-2698.
62. Rueda-Larraz, L., D'arlas, B. F., Tercjak, A., Ribes, A., Mondragon, I. & Eceizaa, A. (2009) Synthesis and microstructure-mechanical property relationships of segmented polyurethanes based on a PCL-PTHF-PCL block copolymer as soft segment. *European Polymer Journal* **45(7)**:2096-2109.
63. Dorin, R. M., Sai, H. & Wiesner, U. (2014) Hierarchically Porous Materials from Block Copolymers. *Chemistry of Materials* **26(1)**:339-347.
64. Lim, L. T., Auras, R. & Rubino, M. (2008) Processing technologies for poly(lactic acid). *Progress in Polymer Science* **33(8)**:820-852.
65. Lizundia, E. Larrañaga, A., Vilas, J.L., & León, L. M. (2016) Three-dimensional orientation of Poly(L-lactide) crystals under uniaxial drawing. *RSC Advances* **6(15)**:11943-11951.
66. Zhao, Z. X., Yang, L., Hu, Y. F., He, Y., Wei, J. & Li, S. M. (2007) Enzymatic degradation of block copolymers obtained by sequential ring opening polymerization of L-lactide and epsilon-caprolactone. *Polymer Degradation and Stability* **92(10)**:1769-1777.
67. Li, S., A.Girard, Garreau, H. & M.Vert (2001). *Polymer Degradation and Stability* **71**:61-67.